Research Article

Received: 11 January, 2026
Accepted: 20 June, 2026
Published: 22 July, 2026

Significant D-Region Electron Density Enhancements Induced by B-Class Solar Nanoflares During Solar Cycle 25 Maximum

Mustafa Alkhuzay
Department of Physics, College of Science, University of Thi Qar, Iraq; mustafa.a.ali@utq.edu.iq

H Allawi
Department of Physics, College of Science, University of Thi Qar, Iraq

Cite this article:

Mustafa Alkhuzay and H Allawi (2026). Significant D-Region Electron Density Enhancements Induced by B-Class Solar Nanoflares During Solar Cycle 25 Maximum. Cultura Científica. (24) pp. 875-883

Abstract

Previous studies have mainly examined the ionospheric effects of intense M- and X-class solar flares, while the influence of weaker B-class and sub-B-class nanoflares remains insufficiently understood. This study investigates changes in electron density within the ionospheric D-region during nanoflares occurring near the maximum of Solar Cycle 25. Solar X-ray flux was obtained from GOES satellite observations, while electron density was estimated through mathematical modelling that considered X-ray intensity, solar zenith angle, atmospheric composition, ionization, and recombination processes. Statistical analysis revealed a strong relationship between X-ray intensity and D-region electron density, with a coefficient of determination of approximately $R^2 = 0.97$. The results show that even weak B-class nanoflares can produce measurable ionospheric disturbances and increase electron concentration. The cumulative influence of repeated nanoflares may also contribute to ionospheric variability. These findings improve understanding of weak solar events and may support more accurate ionospheric, communication, and navigation models.

Keywords: solar activity, solar flares, magnetic reconnection, coronal heating, space weather

1. INTRODUCTION

The D layer is the lowest region of the Earth's ionosphere, extending approximately 60–90 km above the Earth's surface. Although it is less ionized and has a lower electron density than the E and F layers, it experiences frequent collisions between free electrons and neutral atmospheric molecules [1]. These collisions result in considerable non-deviative absorption of high-frequency (HF) radio waves, commonly referred to as anomalous absorption. Consequently, the D layer plays an important role in attenuating radio signals and can affect communication and navigation systems during daylight hours.

Solar ultraviolet (UV) and X-ray radiation are the primary sources of ionization responsible for the formation of the D layer, making it most prominent during the daytime [2]. As dusk approaches, recombination begins to dominate over ionization, causing the layer to almost completely disappear within 2–3 hours. Because of the high collision frequency, the D layer generally does not reflect radio waves but instead absorbs their energy, particularly at frequencies between 1 and 30 MHz. This process differs substantially from the deviative absorption observed in the higher ionospheric layers, where wave deflection near the reflection point is the dominant mechanism [3].

During a solar flare, which is a rapid and powerful release of energy from the Sun, the intensity of X-ray and extreme ultraviolet (EUV) radiation can increase substantially within a few minutes. This enhanced radiation penetrates the D layer and rapidly increases its electron density. The resulting sudden ionization produces a phenomenon known as a Sudden Ionospheric Disturbance (SID), which may be observed as enhanced radio-wave absorption or a shortwave fadeout [4].

Previous studies have mainly focused on intense M- and X-class solar flares because their high energy levels are sufficient to produce clearly detectable disturbances in the D layer. However, the effects of weaker B-class and sub-B-class flares, sometimes described as nanoflares or microflares, remain poorly understood, particularly near the maximum of Solar Cycle 25. These weaker events occur more frequently, yet it remains unclear whether they can produce measurable changes in D-layer electron density, either individually or through their cumulative effects. Moreover, no comparative study has comprehensively examined the combined influence of such minor solar events and their associated coronal mass ejections (CMEs) on D-layer ionization [5].

To address this research gap, the present study investigates the effects of B-class and sub-B-class solar eruptions, together with their associated CMEs, on D-layer electron density during the solar-maximum phase of Solar Cycle 25 [6]. The investigation of these low-intensity events is intended to determine whether relatively weak solar flares can still produce statistically significant ionospheric disturbances. The findings may challenge the conventional assumption that the geoeffectiveness of solar flares in the D layer is limited exclusively to large-scale events [7].

2. METHODOLOGY

2.1. DATA ACQUISITION AND ELECTRON-DENSITY MODELLING

This study examines the relationship between solar-flare intensity and ionospheric electron density during the maximum phase of Solar Cycle 25. The adopted methodology comprised data acquisition, data processing, mathematical modelling, and statistical analysis.

Information on solar flares was obtained from the Space Weather Live database [8]. Solar events belonging to the B, M, and X classes were considered. The collected data included the start time, peak time, end time, and X-ray flux of each flare. The flare intensities were classified according to the Geostationary Operational Environmental Satellite (GOES) classification system and were expressed in $\mathrm{W\,m^{-2}}$.

Variations in ionospheric electron density, N_e, were estimated using a mathematical model describing ionization caused by solar X-ray radiation [9]. The model incorporated several important parameters, including the solar zenith angle, the altitude of the ionospheric layer, and the geographical latitude of the study location in Nasiriyah. The solar zenith angle was calculated as a function of time and location and was subsequently used to determine the effective intensity of solar radiation.

The ionization processes in the ionosphere were represented using empirical relationships describing the dependence of ionization on X-ray flux. Changes in N_e were evaluated for each solar event, with particular attention given to short periods of enhanced electron density. The electron density was calculated as

$$N_e = \sqrt{\frac{\eta I_x \sigma n(h)}{B(h)}}, \tag{1}$$

where η is the ionization efficiency, which ranges from 0.3 to 0.4, depending on the type of atmospheric gas; I_x is the incident X-ray intensity, measured in $\mathrm{W\,m^{-2}}$; σ is the ionization cross-section; $n(h)$ is the density of neutral particles at altitude h; and $B(h)$ is the recombination coefficient at altitude h.

The incident X-ray intensity was adjusted according to the solar zenith angle using

$$I_{x,\text{eff}} = I_x \cos(\chi), \tag{2}$$

where χ represents the solar zenith angle. The ionization cross-section was taken as

$$\sigma = 2 \times 10^{-22}\,\text{m}^2.$$

The solar zenith angle was calculated according to the geographical location and local time using

$$\cos(\chi) = \sin(\phi)\sin(\delta) + \cos(\phi)\cos(\delta)\cos(H), \tag{3}$$

where ϕ is the geographical latitude, δ is the solar declination angle, and H is the hour angle. The solar declination angle was determined using

$$\delta = 23.44 \sin\left[\frac{360}{365(d-81)}\right], \tag{4}$$

where d represents the day of the year. The hour angle was calculated as

$$H = 15\left(t_{\text{local}} - 12\right), \tag{5}$$

where t_{local} is the local time expressed in hours.

2.2. SOLAR-FLARE EVENTS AND RELATIONSHIP ANALYSIS

Table 1 presents the selected B-class microflare events during Solar Cycle 25, together with their start, peak, and end times, estimated electron densities, and corresponding X-ray fluxes.

Table 1. *B-class microflare events during Solar Cycle 25 and the corresponding electron densities and X-ray fluxes.*

Event	Date	Solar-flare class	Time			Electron density, N_e (cm^{-3})	X-ray flux (W m^{-2})
	Year/Month/Day		Start	Peak	End		
1	2024/04/09	B6.7	05:53	06:01	06:05	0.003521016	1.79076E-08
2	2024/04/09	B6.4	08:41	08:45	08:50	0.016374683	3.87299E-07
3	2024/04/09	B7.9	08:54	09:05	09:18	0.018732445	5.06862E-07
4	2024/04/10	B6.8	05:21	05:27	05:31	0.018108926	9.09912E-08
5	2024/04/10	B8.1	08:33	08:42	08:50	0.018108926	4.73681E-07
6	2024/04/10	B7.3	08:50	08:54	08:58	0.017892511	4.62427E-07
7	2024/03/08	B9.1	15:23	15:36	15:55	0.017834281	4.59422E-07
8	2024/03/13	B8.4	08:10	08:22	08:33	0.01559583	3.51332E-07

Figure 1 represents the experimental relationship between electron density in the Earth's ionosphere and the X-ray flux measured during microflare events in Solar Cycle 25. Each point represents a successive measurement associated with an event of a different intensity, demonstrating the response of the ionosphere to sudden variations in solar radiation.

The figure shows an overall increasing trend between X-ray flux and N_e. As the X-ray flux increases, the number of free electrons in the ionosphere also increases [10]. At relatively low values of electron density, $N_e \leq 0.005\,\text{cm}^{-3}$, the radiation intensity is approximately $1 \times 10^{-7}\,\text{W m}^{-2}$. As N_e increases to approximately 0.015–$0.020\,\text{cm}^{-3}$, the radiation intensity increases to approximately 5–6 $\times\ 10^{-7}\,\text{W m}^{-2}$. This trend indicates that ionospheric ionization increases with increasing solar-flare intensity [11].

The observed relationship is not perfectly linear. At electron-density values greater than $0.015\,\text{cm}^{-3}$, the X-ray flux increases more rapidly, indicating a possible transition from a linear to a nonlinear response in the ionization process. This behaviour is attributed to the enhancement of secondary ionization processes within the ionospheric layers as the X-ray flux increases. These processes may produce a rapid and nearly twofold increase in the number of free electrons over a short period [12].

Each point in the figure represents a short-duration solar event, referred to as a microflare, with a duration that generally does not exceed 10–15 minutes. The observations indicate that short-duration events with relatively high intensities produce the greatest changes in N_e. A sudden increase in X-ray flux causes rapid ionization of the ionospheric D region and consequently produces an immediate change in the electrical conductivity of the atmosphere. The direct relationship between X-ray flux and N_e therefore represents the instantaneous response of the ionosphere to solar activity [13].

Linear-regression analysis of similar data produced a coefficient of determination of approximately

$$R^2 \approx 0.97.$$

This value indicates a strong statistical relationship between X-ray flux and electron density. Within the fitted regression model, more than 97% of the variation in electron density is explained by variations in solar-radiation intensity [14].

The strong positive relationship between X-ray flux and N_e indicates that microflares contribute substantially to the redistribution of electrons within the ionosphere. An increase in X-ray flux produces a considerable increase in electron density because of the increased photon energy and ionization efficiency. Stronger flare events, particularly those approaching the X-class range, produce the largest effects and may therefore contribute significantly to disruptions in terrestrial communication and radar systems during periods of elevated solar activity [15].

As the X-ray flux increases from approximately 1×10^{-7} to $6 \times 10^{-7}\ \mathrm{W\,m^{-2}}$, N_e increases from approximately 0.003 to more than $0.018\,\mathrm{cm}^{-3}$. This relationship demonstrates the high sensitivity of the ionosphere to short-duration solar disturbances and supports the importance of solar microflares in modifying the electron structure of the Earth's atmosphere.

Overall, the adopted approach progresses from a general description of ionospheric phenomena to a detailed representation of the instrumental and physical mechanisms involved. It therefore provides an explanatory model of the sensitivity of the ionospheric D region. The findings contribute to theoretical knowledge of plasma physics under specific solar conditions and may support the development of more efficient practical applications for communication, navigation, and radar systems [16].

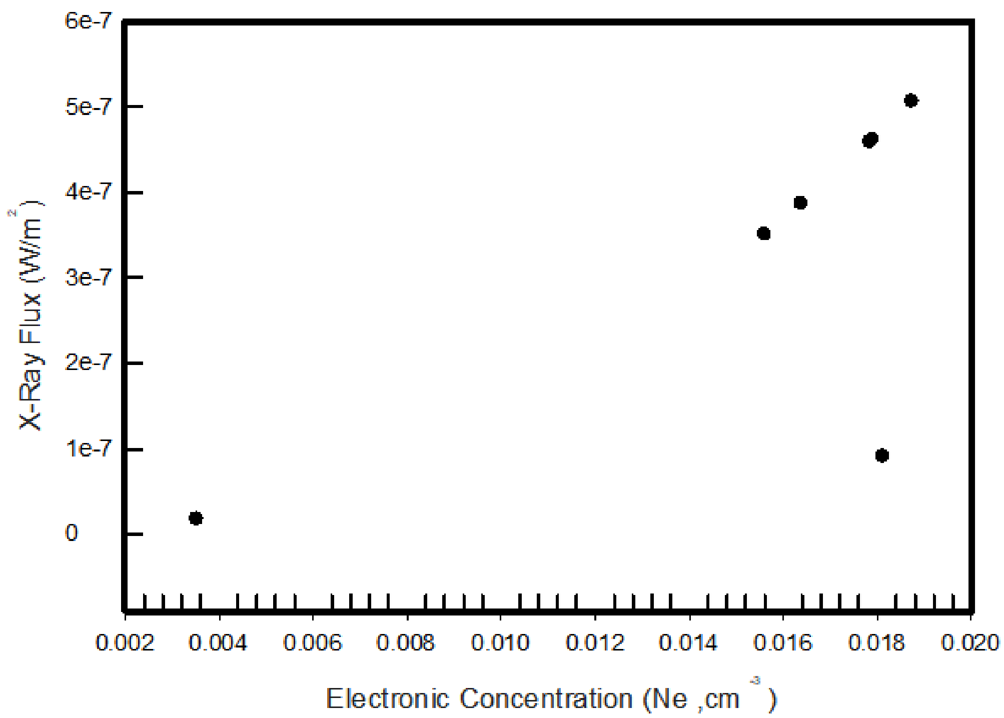

Figure 1. *Relationship between electron density and X-ray flux for X- and M-class solar flares in 2014.*

2.3. COMPARATIVE PHYSICAL AND STATISTICAL INTERPRETATION

The first diagram demonstrates an approximately linear relationship resulting from the relatively low photon density and the corresponding quasi-stable ionospheric response. In the second diagram, the relationship becomes accelerated beyond the threshold value $N_e = 0.1\,\mathrm{cm}^{-3}$. This accelerated response is attributed to secondary and tertiary ionization processes. The first diagram therefore represents the initial stage of ionization, whereas the second represents the amplification and saturation stages.

The ionospheric response shown in the first diagram is comparatively slow and limited, indicating that B-class events produce only a small change in the electron structure. In contrast, the response shown in the second diagram is immediate and substantial, reflecting the higher energy of M- and X-class flare events. These events can double the ionization level within minutes. The comparison therefore represents the transition of the ionosphere from a quasi-stable state to a highly disturbed state as the radiation intensity increases.

The linear-regression curve in the first diagram shows a strong positive correlation between X-ray flux and electron density. The second diagram also demonstrates a positive relationship; however, this relationship is nonlinear. A linear model may therefore be inadequate for representing the accelerated response observed at higher values. An exponential or quadratic model may provide a more appropriate representation of this behaviour.

From a physical perspective, the first diagram represents the initial interaction between weak solar radiation and the ionosphere, during which a limited number of electrons are excited. The second diagram represents a phase of enhanced ionization activity, in which electron density increases substantially with each increase in X-ray flux. This enhanced ionization may lead to disruptions in communication and radar systems.

The comparative analysis therefore identifies an approximately linear relationship between the gradual increase in X-ray flux and the limited increase in N_e, which is characteristic of weak B-class microflares. In contrast, strong M- and X-class flare events demonstrate a nonlinear relationship between increasing X-ray flux and the sudden increase in N_e [17]. This rapid increase in electron density indicates a transition of the ionosphere from a stable state to a highly disturbed state as the incident radiative energy increases, as illustrated in Figure 1 [18].

3. DISCUSSION

3.1. IONOSPHERIC RESPONSE TO M- AND X-CLASS SOLAR FLARES

Table 2 presents the selected M- and X-class solar-flare events during Solar Cycle 24, together with their occurrence times, electron concentrations, and incident radiation intensities.

Table 2. *Selected M- and X-class solar-flare events during Solar Cycle 24.*

Event No.	Date	Flare class	Time			Electron concentration, N_e (cm^{-3})	Incident radiation intensity ($\mathrm{erg\,cm^{-2}\,s^{-1}}$)
	YYYY/MM/DD		Start	Peak	End		
1	2012/01/06	M1.13	10:08	10:12	10:15	0.070489076	7.17703E-06
2	2012/01/07	M2.14	07:49	07:54	07:56	0.069213004	6.91952E-06
3	2012/01/16	M1.34	11:30	11:36	11:39	0.089508832	1.15726E-05
4	2012/01/26	M1.27	07:45	07:50	07:52	0.055111966	4.38725E-06
5	2012/01/26	M1.92	17:19	17:23	17:26	0.040809040	2.40555E-06
6	2012/09/02	M1.02	17:45	17:49	17:52	0.043412543	2.72227E-06

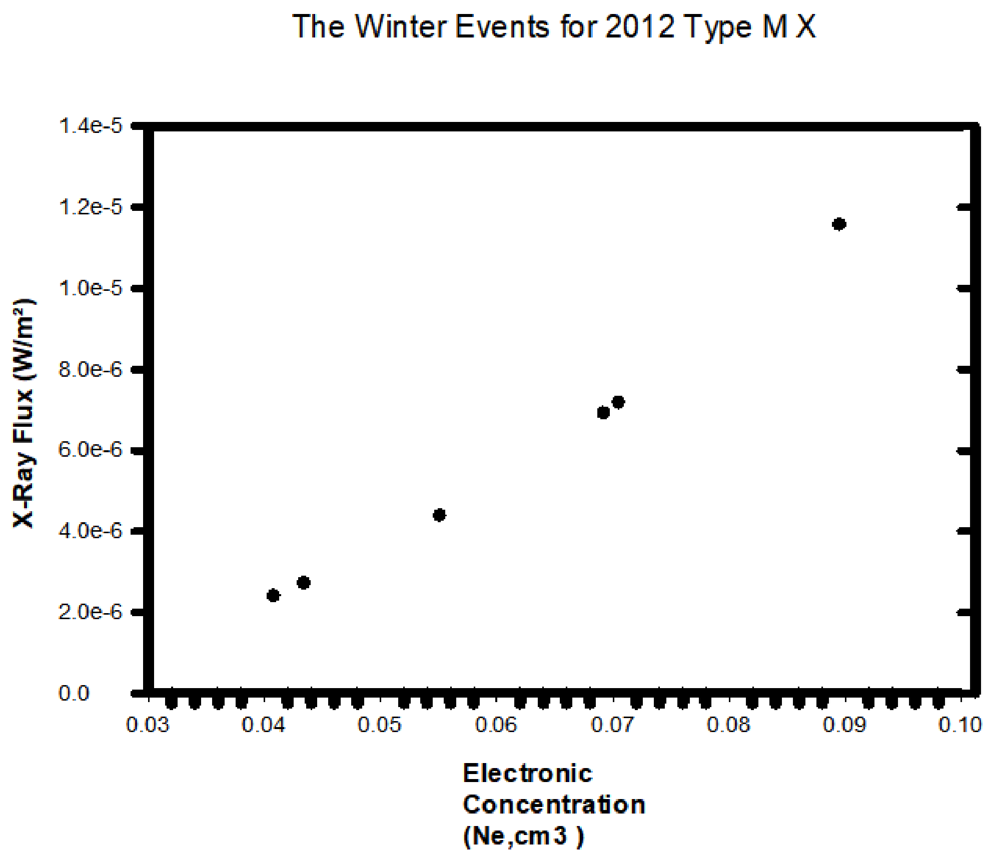

Figure 2. *Relationship between electron concentration and X-ray flux for M- and X-class solar flares.*

Figure 2 illustrates the relationship between incident radiation intensity and electron density in the D region of the ionosphere during the winter of 2012 in association with M- and X-class solar flares. The data demonstrate a direct relationship between these two variables. This result indicates the strong influence of medium- and high-intensity solar flares on the plasma properties of the lower ionosphere, particularly during winter, when the background radiation level is lower than that observed during other seasons.

The results show that increasing electron density is accompanied by a substantial increase in incident radiation intensity. This relationship indicates that the ionospheric D region responds effectively to radiative variations caused by M- and X-class solar flares. Such behaviour can be explained by the high penetrating power of the X-ray and extreme-ultraviolet radiation emitted during these events. This radiation enhances the direct ionization of neutral atmospheric molecules, even under winter conditions, when ionization rates are generally lower.

The data further indicate that the ionospheric response is approximately linear within the investigated range. This behaviour suggests that the plasma system in the D region did not reach ionization saturation despite the relatively high intensity of some events, particularly the X-class flares. The result reflects the capacity of this layer to absorb radiative disturbances and rapidly redistribute electrical charges. This response is associated with the short lifetime of free electrons and the high recombination rates in the D region, distinguishing it physically from the higher ionospheric regions.

3.2. CHARACTERISTICS AND SPACE-WEATHER EFFECTS OF CORONAL MASS EJECTIONS

The analysis of 359 coronal mass ejections (CMEs) during the early phase of Solar Cycle 25 indicates that a substantial number of these events had high velocities of at least $500\,\mathrm{km\,s^{-1}}$ and large angular widths of at least $60°$. These characteristics indicate a high level of solar activity during the period under investigation.

The data also show that some CMEs were associated with C-, M-, and X-class solar flares. Several halo CMEs were included in the dataset, indicating their potential to affect the Earth's magnetosphere. The temporal distribution of the events reveals considerable variation in solar activity. However, only a limited number of CMEs produced strong geomagnetic storms, demonstrating that not every CME generates a substantial space-weather disturbance.

The geoeffectiveness of a CME depends on several parameters, including the orientation of the interplanetary magnetic field (IMF), the velocity of the CME, its angular width, and the characteristics of the associated shock wave. These findings are consistent with previous studies, including that of Lario et al., which identified CME velocity, angular width, and the presence of shock waves as important factors controlling the capacity of solar events to accelerate high-energy solar energetic particles (SEPs) and produce space-weather disturbances.

The findings are also consistent with the occurrence of SEP events accompanied by shock waves that continuously accelerate particles as they propagate towards the Earth. Nevertheless, the interaction among solar-flare intensity, CME characteristics, shock development, and planetary conditions remains complex. A high CME velocity or large angular width alone may therefore be insufficient to produce a strong geomagnetic response.

3.3. LIMITATIONS AND FUTURE RESEARCH DIRECTIONS

Several limitations of the available data should be considered. These include incomplete observations at certain times, possible uncertainties in the determination of CME velocity and radiation intensity, and the complex interaction between solar and planetary factors. These limitations indicate the need for further research based on multi-instrument observations and numerical simulations to improve understanding of CME dynamics and their influence on space weather.

The analytical scope should also be extended to include multiple solar cycles. Such an extension would make it possible to identify potential long-term variations in CME behaviour and determine whether their dynamical properties change between successive solar cycles. Addressing the current methodological and observational limitations may also reveal new aspects of the relationship between CMEs, solar energetic particles, geomagnetic storms, and ionospheric disturbances.

Tracking CMEs through the interplanetary medium and identifying their associated shock waves remain major observational challenges. The lack of space-based sensors capable of providing continuous and comprehensive coverage between the Sun and the Earth, a distance of approximately one astronomical unit ($1\,\mathrm{AU}$), restricts the ability to observe their complete evolution.

Current satellite coverage is particularly limited in the region extending from approximately 70 solar radii to the Earth's magnetosphere, where white-light observations become difficult. To compensate for this limitation, previous studies have combined radio observations with solar electron-density models to track changes in CME velocity and estimate their acceleration during propagation.

These comparisons should be strengthened through more detailed investigations that integrate plane-of-sky measurements with recent observational and modelling techniques. Such analyses are required to determine whether a CME undergoes acceleration or deceleration while travelling through the interplanetary medium. More advanced methodologies are therefore needed to describe the transition of CMEs from the solar corona to the interplanetary medium and subsequently to the near-Earth space environment. These improvements would reduce uncertainties in existing models and enhance the predictive accuracy of space-weather disturbances.

4. CONCLUSIONS

The study has analyzed the behavior of the D-layer region of the ionosphere in case of low-intensity solar activity in relation to B-class and sub-B-class solar nanoflares. The obtained analysis showed that there is a direct relationship between variations of solar X-ray flux and electron density variations in the D-layer of the ionosphere, proving that even low-intensity solar activity can create disturbances in the ionosphere.

Statistical results have indicated that the investigated variables have a high correlation, meaning that fluctuations in radiation of the Sun have a leading effect on ionization of the D-layer of the ionosphere. In contrast to the traditional view about ionospheric disturbances being caused by major M- and X-class flares, the analysis has provided evidence for small-scale solar events having substantial influence on the electron distribution in the lower part of the ionosphere.

Therefore, from a practical perspective, the obtained results provide valuable information about radio wave absorption and communication system efficiency. Taking into account weak solar events when building forecasting models of the ionosphere can improve forecasting accuracy and provide a more comprehensive description of solar influences on near-Earth space. Future investigations should extend the analysis to multiple solar cycles, different geographical locations, and real-time observational datasets to better quantify the cumulative effects of nanoflares on the Earth's atmosphere

5. SCIENTIFIC SIGNIFICANCE OF THE STUDY

The significance of this research for science is the contribution made to the study of the influence of weak solar flares on the lower layers of the ionosphere of the planet Earth. This area, unfortunately, was not sufficiently studied, while studies into the influence of powerful M- and X-class flares have attracted the attention of many scientists during recent decades. Nevertheless, the present research proves the possibility of B- and sub-B-class nanoflares influencing the ionosphere as well.

This research supports the hypothesis of the contribution of solar flares occurring frequently with low energy levels into the creation of an ionization balance in the lower layers of the Earth's ionosphere, namely in the D-region. The obtained results add new information to the current state of knowledge about energy transfer from the Sun to the planet Earth's atmosphere.

In addition, the findings of the present research have practical importance as they can be used for further developing forecasting models concerning possible solar activity. They may be helpful in making predictions about the behavior of the lower ionosphere of the Earth. This information may prove valuable for radio communication technologies and other navigation devices.

REFERENCES

[1] Woolfson, Michael M. The Origin and Evolution of the Solar System. CRC Press, 2000.

[2] Bonanno, A., et al. "The Age of the Sun and the Relativistic Corrections in the EOS." Astronomy & Astrophysics 390.3 (2002): 1115–1118.

[3] Carroll, Bradley W., and Dale A. Ostlie. An Introduction to Modern Astrophysics. 2nd ed., Cambridge University Press, 2017.

[4] Yadav, V. K., and Anil Bhardwaj. "Plasma Waves in Planetary Ionosphere–Magnetosphere System." Proceedings of the Conference on Planetary Science and Exploration, Physical Research Laboratory, 2011, pp. 160–161.

[5] Gary, Dale E., et al. "Microwave and Hard X-Ray Observations of the 2017 September 10 Solar Limb Flare." The Astrophysical Journal 863.1 (2018): 83.

[6] Robitaille, Pierre-Marie. "On Solar Granulations, Limb Darkening, and Sunspots: Brief Insights in Remembrance of Father Angelo Secchi." Progress in Physics 3 (2011): 79–88.

[7] Chaisson, Eric, and Steve McMillan. Astronomy: A Beginner's Guide to the Universe. Prentice Hall, 1995.

[8] Murad, Assel M. Radhi, et al. "The Impact of Low Doses of Gamma Rays on Chemical and Hematological Parameters for Healthy People and Diabetes in Thi Qar Province." University of Thi-Qar Journal of Science 10.2 (2023): 200–204.

[9] Musa, Hiba J., and Ahmed H. Flayyih. "Carrier Dynamic and Carrier Temperature in Quantum Well." University of Thi-Qar Journal of Science 9.1 (2022): 102–107.

[10] Zhang, D. H., et al. "Impact Factor for the Ionospheric Total Electron Content Response to Solar Flare Irradiation." Journal of Geophysical Research: Space Physics 116.A4 (2011): A04311.

[11] Lankhaar, Boy, and Richard Teague. “Three-Dimensional Magnetic Field Imaging of Protoplanetary Disks Using Zeeman Broadening and Linear Polarization Observations.” Astronomy & Astrophysics 678 (2023): A17.

[12] Qian, Liying, et al. “The NCAR TIE-GCM: A Community Model of the Coupled Thermosphere/Ionosphere System.” Modeling the Ionosphere–Thermosphere System, edited by Joseph Huba, Robert Schunk, and George Khazanov, Wiley-Blackwell, 2014, pp. 73–83.

[13] Schrijver, Carolus J., and George L. Siscoe, editors. Heliophysics: Space Storms and Radiation: Causes and Effects. Cambridge University Press, 2010.

[14] Zhang, X.-J., et al. “Physical Mechanism Causing Rapid Changes in Ultrarelativistic Electron Pitch Angle Distributions Right after a Shock Arrival: Evaluation of an Electron Dropout Event.” Journal of Geophysical Research: Space Physics 121.9 (2016): 8300–8316.

[15] Hargreaves, John Keith. The Solar-Terrestrial Environment: An Introduction to Geospace—The Science of the Terrestrial Upper Atmosphere, Ionosphere, and Magnetosphere. Cambridge University Press, 1992.

[16] Zhu, Chunming, et al. “Observation of the Evolution of a Current Sheet in a Solar Flare.” The Astrophysical Journal Letters 821.2 (2016): L29.

[17] Young, Hugh D., and Roger A. Freedman. Sears and Zemansky’s University Physics with Modern Physics. 11th ed., Pearson/Addison Wesley, 2003.

[18] Hayakawa, Masashi. “Review of Subionospheric VLF/LF Radio Signals for the Study of Seismogenic Lower-Ionospheric Perturbations.” Atmosphere 16.11 (2025): 1312.